Traps and performance of MEH-PPV/CdSe(ZnS) nanocomposite-based organic light-emitting diodes

2008 Nanotechnology 19 455202

(http://iopscience.iop.org/0957-4484/19/45/455202)

Nanotechnology **19** (2008) 455202 (7pp) doi:10.1088/0957-4484/19/45/455202

Traps and performance of MEH-PPV/CdSe(ZnS) nanocomposite-based organic light-emitting diodes

Chih-Wen Lee[1,2], Cedric Renaud[1], Chain-Shu Hsu[2] and Thien-Phap Nguyen[1]

[1] Institut des Matériaux Jean Rouxel, Université de Nantes-CNRS, 2 rue de la Houssinière, BP32229, 44322 Nantes, France
[2] Department of Applied Chemistry, National Chiao Tung University, Hsinchu 30010, Taiwan

E-mail: nguyen@cnrs-imn.fr

Received 17 July 2008, in final form 2 September 2008
Published 8 October 2008
Online at stacks.iop.org/Nano/19/455202

Abstract

We report the fabrication and investigations of organic light-emitting diodes (OLEDs) using a composite made by mixing poly[2-methoxy-5(2′-ethylhexyloxy)-1,4-phenylenevinylene] (MEH-PPV) with CdSe/ZnS core/shell quantum dots (QDs). The electroluminescence efficiency of the studied devices was found to be improved as compared to devices using MEH-PPV. Moreover, the current density decreased with increasing QD concentration. We checked the effects of QDs on the electrical transport by determining the trap states, making use of the charge-based deep level transient spectroscopy (Q-DLTS) technique. The most striking result obtained is the decrease in trap density when adding QDs to the MEH-PPV polymer film. These results suggest that QDs would heal defects in nanocomposite-based devices and that CdSe/ZnS QDs prevent the trap center formation.

(Some figures in this article are in colour only in the electronic version)

1. Introduction

Since the first demonstration of polymer light-emitting diodes in 1990 [1, 2], considerable progress has been made in the organic semiconductor field, and applications are currently reaching the commercialization stage in organic light-emitting devices (OLEDs). Conjugated polymers and molecules are used as active elements in these devices and they provide many advantages such as easy fabrication, low cost, good processability and large surface for possible applications in flat panel display technology [3, 4].

At the same time, developments in semiconductor nanotechnology have led to new materials having specific properties, which can be considered for electronic applications because of their strong quantum size confinement effects. In particular, colloidal semiconductor nanocrystal quantum dots (QDs) have attracted wide attention due to their tuneable emission spectra with particle sizes [5, 6]. Furthermore, they also exhibit a high photostability, narrow emission line widths (<30 nm) and a high luminescence efficiency [7, 8]. Incorporating QDs into organic optoelectronic components make them promising candidates for light-emitting diodes [9–13] and photovoltaic cells [14–17].

Among these materials, much research has combined II–VI semiconductor nanoparticles, such as cadmium selenium (CdSe) and cadmium sulfide (CdS), with organic materials to fabricate OLEDs [18–20]. Hybrid materials made of QDs and a conjugated polymer are usually used in multilayer structures, in which the organic material is deposited as a hole transport layer (HTL) [20]. Two possible processes may take place in a composite film. In the first process, the injected electrons and holes recombine inside the QD layer, whenever this latter can be formed in the active layer. In this case, the emitted light comes from the QDs. The second process involves

recombination of excitons inside the organic layer. The emitted light comes from the polymer, and the QDs are added to the host matrix to improve the device efficiency. Generally speaking, the enhancement of the performance is due either to a better charge injection [21–24] or to an energy transfer from QDs to the electroluminescent material [25]. However, when a QD layer is formed inside the film from a phase separation in the composite [26], it can block the injected holes and electrons by high-energy barriers that are formed in the emitting layer, and allows a balance in the charge transport, thus improving the device performance.

In this paper, we describe the fabrication of hybrid devices using nanocomposites made by incorporating CdSe/ZnS core/shell QDs to poly(2-methoxy-5(2′-ethylhexoxy-phenylenevinylene) (MEH-PPV). We found that the performance of devices is significantly improved by QD incorporation, and in order to understand the effects of QDs in the transport process we studied the defect states of the hybrid material by charge-based deep level transient spectroscopy (Q-DLTS). This technique provides the trap parameters of the active layers. From analysis of results obtained in devices with and without QDs, we shall discuss the influence of QDs on the trap parameters and we relate them to the performance of the structures.

2. Experimental details

CdSe/ZnS core–shell QDs passivated with trioctylphosphineoxide (TOPO) caps were synthesized according to a procedure reported previously [27]. They were incorporated into an MEH-PPV solution of concentration 10 mg ml^{-1} dissolved in toluene. The absorption spectra of thin films were measured with a Cary 5G spectrophotometer and the photoluminescence (PL) spectra were obtained with a Fluorolog Horiba spectrophotometer. Transmission electron microscopy (TEM) observation was carried out using a Hitachi H-9000-NAR electron microscope, operating at 300 kV.

Devices were fabricated as sandwich structures between an aluminum cathode and an indium tin oxide (ITO) anode. ITO-coated glass substrates were cleaned sequentially in ultrasonic baths of detergent, 2-propanol/deionized water (1:1 volume) mixture, toluene, deionized water and acetone. A 50 nm thick hole injection layer of poly(ethylenedioxythiophene) (PEDOT) doped with poly(styrenesulfonate) (PSS) was spin-coated on top of ITO substrates from a 0.7 wt% dispersion in water and was dried at 150 °C for 1 h in vacuum. The pristine MEH-PPV or MEH-PPV/QDs films were obtained by spin-coating of toluene solutions onto the PEDOT layer and were dried at 80 °C in vacuum. Finally, a 100 nm Al electrode was deposited through a shadow mask onto the polymer films by thermal evaporation, using an Auto 306 vacuum coater (BOC Edwards, Wilmington, MA). The evaporations were carried out typically at base pressures lower than 8×10^{-7} mbar. The active area of the devices was 4 mm^2. Current–voltage characteristics of the diodes were measured using a Keithley 2400 source meter, and brightness and efficiency by a Photo Research PR650 spectrometer. Q-DLTS measurements were performed using an automated system, ASMEC-06, supplied by InOmTech Inc., the sample being mounted in a cryostat working in the temperature range from 77 to 500 K.

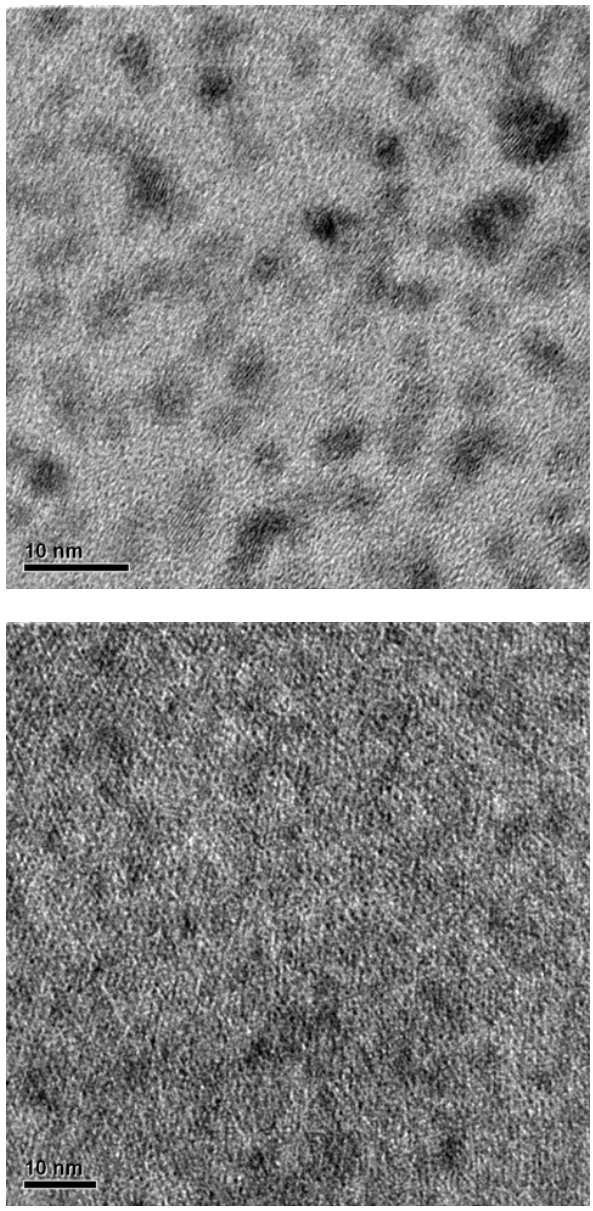

Figure 1. Transmission electron microscopy image of (a) CdSe/ZnS nanoparticles and (b) MEH-PPV/QD composite.

3. Results and discussion

For TEM experiments, polymer/QD solutions were spin-coated onto glass substrates to obtain thin films ∼60 nm thick. Figure 1 shows TEM images of CdSe/ZnS nanoparticles and a MEH-PPV/QD composite. The sizes of nanoparticles in both figures are similar and approximately equal to 4–5 nm. Figure 2 shows the absorption and photoluminescence spectra of pristine MEH-PPV and QDs. The pristine MEH-PPV film exhibits an absorption peak at 500 nm, which is attributed to π–π^* transitions, and an emission peak at 585 nm. For the QDs, the absorption peak is located at

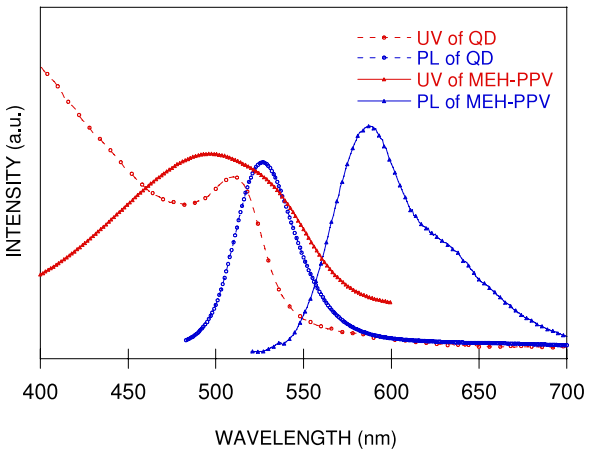

Figure 2. Absorption and photoluminescence spectra of CdSe(ZnS) quantum dots (dashed line) and MEH-PPV polymer (solid line).

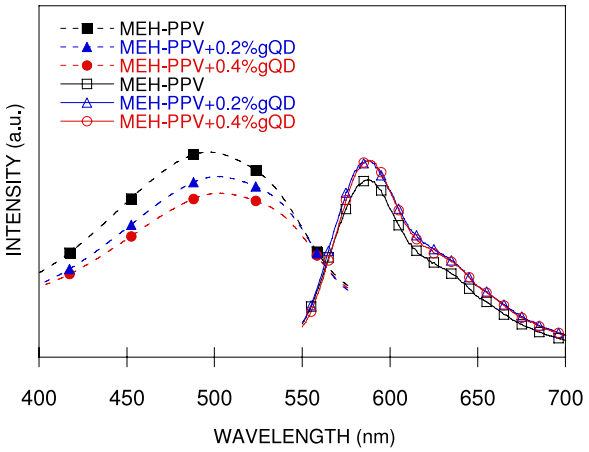

Figure 3. Absorption and photoluminescence spectra of pristine MEH-PPV (■), MEH-PPV + 0.2% QDs (▲), MEH-PPV + 0.4% QDs (●).

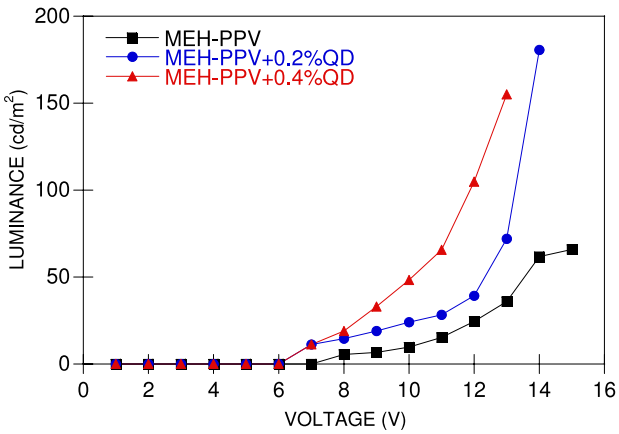

Figure 4. Luminance–voltage characteristics of ITO/PEDOT:PSS/MEH + QDs/Al diodes using MEH-PPV polymer (■), MEH-PPV + 0.2% QDs (●) and MEH-PPV + 0.4% QDs (▲).

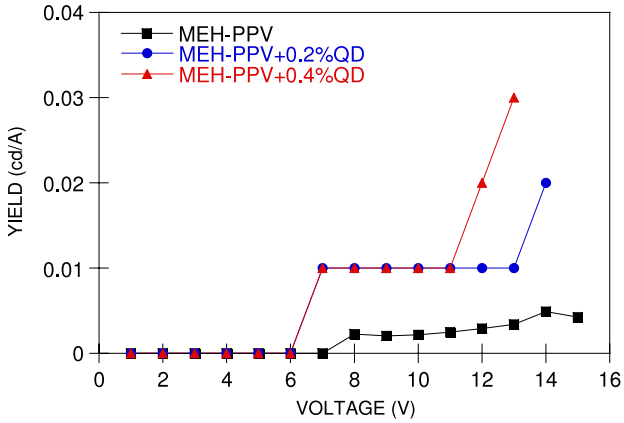

Figure 5. Yield–voltage characteristics of ITO/PEDOT:PSS/MEH + QDs/Al diodes using MEH-PPV polymer (■), MEH-PPV + 0.2% QDs (●) and MEH-PPV + 0.4% QDs (▲).

510 nm and the emission one at 526 nm. The absorption spectra of MEH-PPV/QD composite films shown in figure 3 are found to be similar in shape and position to those of pristine MEH-PPV. These results indicate that the ground-state charge transfer between the polymer and the QDs is negligible, and this can be explained by the fact that the absorption coefficient of the QDs is much smaller than that of MEH-PPV. The excited-state charge-transfer behavior can be investigated by PL measurements. All spectra indicate that polymer luminescence dominates in composites and that the contribution of the QDs is weak. Furthermore, we note that no apparent quenching of luminescence in the composite films was observed. Therefore, a charge transfer from the polymer to the QDs does not occur, contrarily to what is observed in composites having high concentrations of QDs [28, 29]. In our study, very low concentrations of QDs were added to polymer films and there is no overlap between the polymer emission and the QD absorption spectra. Therefore, quenching of polymer luminescence would not happen in the composite systems. On the contrary, the luminescence of the polymer film is slightly increased when QDs are incorporated. This increase can be assigned to an energy transfer between the materials, from the QDs to MEH-PPV, due to the overlap between the emission spectrum of the QDs and the absorption spectrum of the polymer.

Figures 4 and 5 show the luminance and the yield of the diodes as a function of the applied voltage. Incorporation of QDs into the polymer enhances the device luminance from 65 cd m^{-2} to 180 cd m^{-2} and the yield from 0.005 cd A^{-1} to 0.03 cd A^{-1} in pristine MEH-PPV and in MEH-PPV/QDs composite film, respectively. The turn-on voltage also decreases from 8 V in pure MEH-PPV devices to 7 V in composite ones. The electroluminescence (EL) spectra of all devices are found to be similar in shape and position, suggesting that light emission originates from MEH-PPV. This similarity indicates that the same excitation processes occur in the polymer and the composite films. We note that the increase in luminescence is obtained only in devices having low concentrations of QDs (0.4 wt%), and when higher concentrations (>1 wt%) are used, a charge separation in polymer/QD composites occurs, causing a decrease of the EL (not shown). Figure 6 shows the current density as

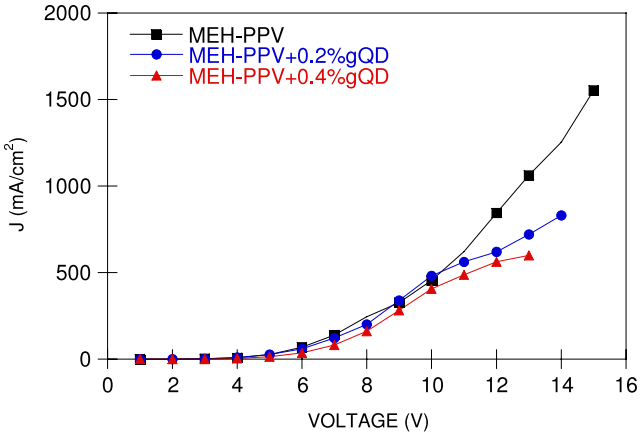

Figure 6. Current–voltage characteristics of ITO/PEDOT:PSS/MEH-PPV + QDs/Al diodes using MEH-PPV (■), MEH-PPV + 0.2% QDs (●) and MEH-PPV + 0.4% QDs (▲).

a function of the applied voltage for devices using MEH-PPV/QD composites (0, 0.2 and 0.4%) as actives layers. The turn-on voltages of the devices are quite similar (6 V), and the current density decreases with increasing QD concentration. The decrease is particularly significant at high applied voltages (>10 V), indicating a modification in the transport processes.

To date, and to our knowledge, there has been no report on the role of CdSe/ZnS QDs in the electrical properties of composite films in relation with their luminescence. Therefore, to further understand the role of the QDs in the electrical transport properties, we have investigated the trap states in pristine polymer and polymer/QD composites by the Q-DLTS technique.

In this technique (figure 7), a voltage pulse ΔV is applied to the sample for a short period of time t_C (charging time) to fill the traps. Complete filling of traps can be obtained when the charging time t_C is correctly chosen. The applied voltage is then set to zero and the trapped charges are released, resulting in a charge movement in the external circuit. A charge ΔQ corresponding to a transient current is measured during a time interval defined by two times t_1 and t_2. It is most convenient to use the time window τ defined by

$$\tau = (t_1 - t_2)/\ln(t_2/t_1). \tag{1}$$

The Q-DLTS spectra are then obtained by plotting the charge transient $\Delta Q = Q(t_2) - Q(t_1)$ as a function of the time window. Assuming that the transient charge is an exponential function of time and providing there is a constant ratio t_2/t_1, the released charges from a discrete trap level without re-trapping can be written as [30–32]

$$Q(t) = Q_0[1 - \exp(-e_{n(p)}t)] \tag{2}$$

where Q_0 is the initial trapped charges during the filling process, and $e_{n(p)}$ is the electron (hole) emission rate at the temperature T, which is given by

$$e_{n(p)} = \sigma\Gamma T^2 \exp(-E_T/kT) \tag{3}$$

where E_T is the activation energy, σ is the capture cross-section, k is the Boltzmann constant and Γ is a constant given by

$$\Gamma = 2 \times 3^{1/2}(2\pi/h^2)^{3/2}k^2 m_{p(n)} \tag{4}$$

where $m_{p(n)}$ is the hole (electron) effective mass. From equation (2) and by using $t_1 = 2t_2$, the charge variation ΔQ as a function of the time window is given by the following relation:

$$\Delta Q = Q_0\left[\exp\left(-\frac{\tau}{\tau_m}\times\ln(2)\right) - \exp\left(-\frac{\tau}{\tau_m}\times 2\ln(2)\right)\right]. \tag{5}$$

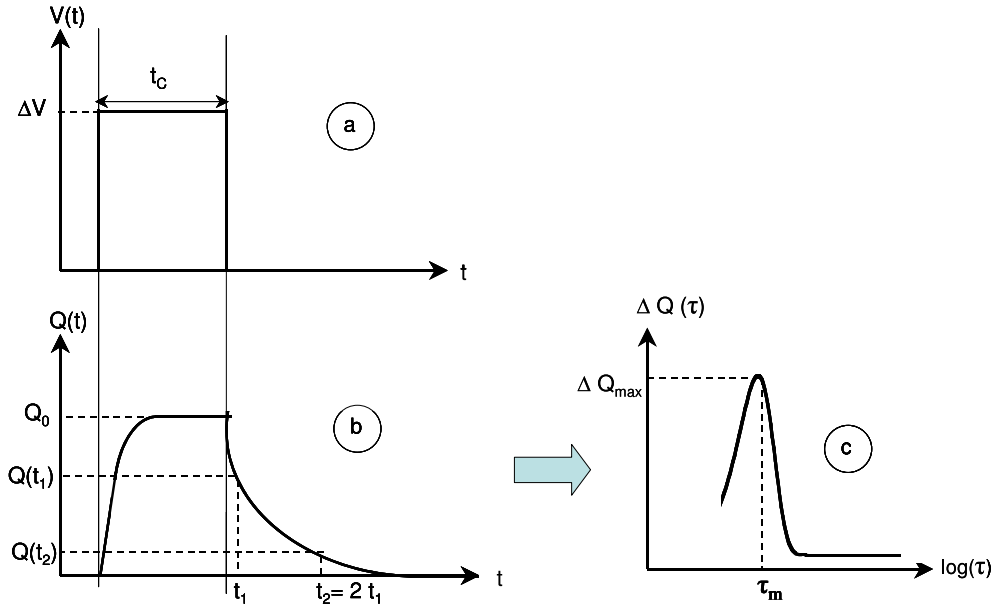

Figure 7. Principle of the Q-DLTS technique: (a) applied voltage, (b) evolution of the charge in the sample, (c) Q-DLTS spectrum.

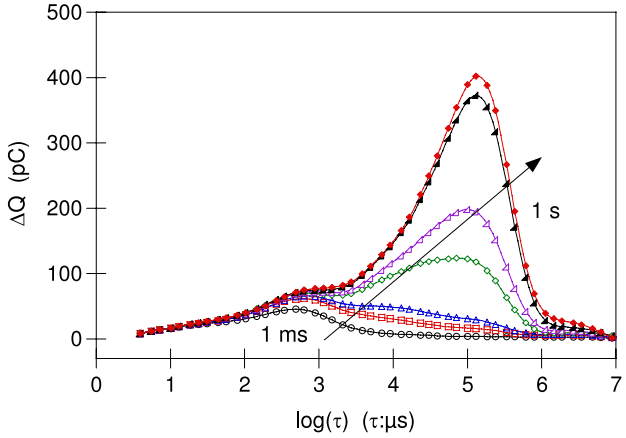

Figure 8. Q-DLTS spectra recorded in an ITO/PEDOT/MEH-PPV/Al diode at 300 K using a charging voltage of $\Delta V = +1$ V for different charging times t_C in the range 1 ms–1 s.

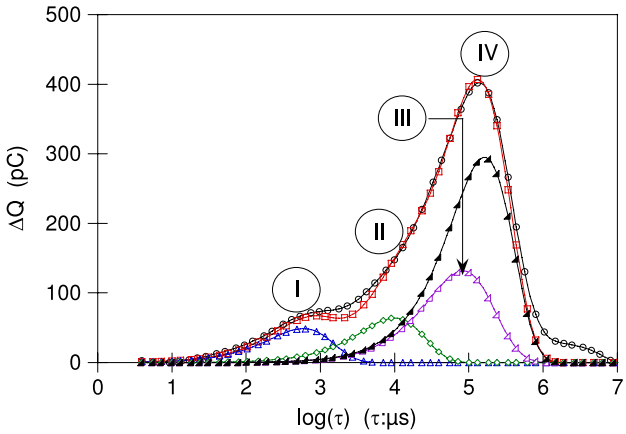

Figure 9. Resolved Q-DLTS spectrum recorded in an ITO/PEDOT/MEH-PPV/Al diode using a charging voltage of $\Delta V = +1$ V, a charging time of $t_C = 1$ s, at 300 K.

It can be demonstrated that the charge variation ΔQ goes through a maximum when the time window τ matches the relaxation time τ_m of the traps at the temperature T [30–32]. Both E_T and σ can then be determined respectively from the slope and intercept of an Arrhenius plot of the form $\ln(eT^{-2})$ versus $1/T$. Furthermore, the trap density N_T can also be calculated from the measurement of the maximum value of the Q-DLTS spectrum and is given by the following relation:

$$N_T = 4\Delta Q_{max}/qAd \tag{6}$$

where q is the electronic charge, A is the contact area, and d is the thickness of the active layer.

Figure 8 shows the Q-DLTS spectra of an ITO/PEDOT:PSS/MEH-PPV/Al structure using a pulse of $\Delta V = +1$ V and different charging times from 1 ms to 1 s at $T = 300$ K. A careful examination of the spectra reveals four peaks, denoted as peaks I, II, III and IV, of relaxation times $\tau_I \sim 0.6$ ms, $\tau_{II} \sim 10$ ms, $\tau_{III} \sim 83$ ms, $\tau_{IV} \sim 158$ ms, respectively. Peak I becomes quickly saturated while peaks II, III and IV are still growing and start to saturate when the charging time t_C equals 1 s. This value is then chosen for recording the spectra. From these results, we resolved the Q-DLTS spectra into four components using equation (5), as shown in figure 9. The parameters of each trap level were determined by recording the Q-DLTS spectra as a function of the temperature. For illustration, figure 10 shows peak I in the temperature range from 250 to 320 K with a charging voltage of $\Delta V = +1$ V. The corresponding Arrhenius curve is displayed in the inset of figure 10. The activation energy obtained from the slope of the curve is 0.20 eV and a capture cross-section of $\sigma = 1 \times 10^{-20}$ cm^2 is determined from the intercept value. From the maximum amplitude of the Q-DLTS peak, the trap density could also be determined to be $N_T \sim 5.2 \times 10^{15}$ cm^{-3}.

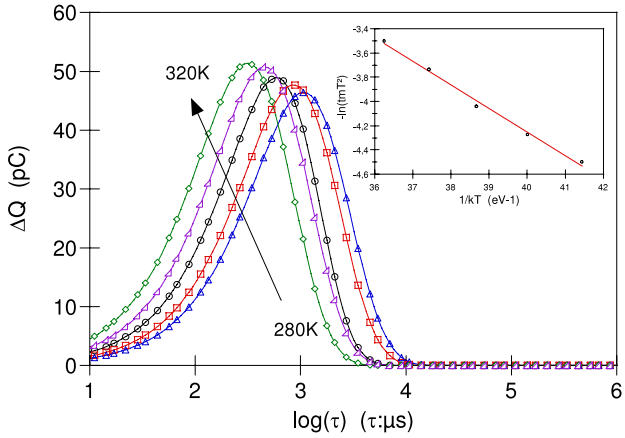

Figure 10. Evolution of Q-DLTS peak I for different temperatures in the range 280–320 K. Inset: corresponding Arrhenius plot.

Table 1. Trap parameters in ITO–PEDOT:PSS–MEH-PPV + QDs–Al diodes. N_{T1}, N_{T2}, N_{T3} are the trap densities in devices with QD concentrations of 0%, 0.2%, 0.4% respectively.

Peaks	E_T (eV)	σ (cm^2)	N_{T1} (cm^{-3})	N_{T2}/N_{T1}	N_{T3}/N_{T1}
I	0.20 ± 0.02	1×10^{-20}	3×10^{15}	0.4	0.3
II	0.30 ± 0.02	1×10^{-19}	4.5×10^{15}	0.7	0.3
III	0.25 ± 0.02	1×10^{-21}	8×10^{15}	0.7	0.3
IV	—	—	2×10^{16}	0.65	0.05
V	0.15 ± 0.02	5×10^{-20}	—	—	—

The trap parameters of an ITO/PEDOT:PSS/MEH-PPV/Al diode are summarized in table 1. We note that the parameters of peak IV could not be determined because this peak does not shift in the temperature range used and is supposed to correspond to deep traps. The activation energies of peaks I, II and III are comparable to those found in previous reports in MEH-PPV-based devices [33–35].

The Q-DLTS spectra of devices using MEH-PPV and 0.4% QDs composite are displayed in figure 11. It can be seen that the amount of relaxed charges decreased in devices using the composites as an active layer. Furthermore, an excess of charges is observed at high relaxation times, suggesting that new trap levels could be formed. The resolved spectrum of the doped device shown in figure 12 clearly displays a new peak, labeled V, of relaxation time $\tau_V \sim 0.69$ s, in addition to the peaks already found in the MEH-PPV device. Therefore, doping the polymer introduced an

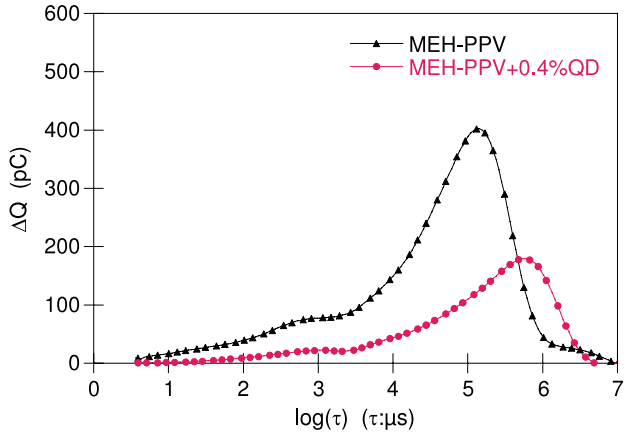

Figure 11. Q-DLTS spectra of diodes using MEH-PPV (▲) and MEH-PPV + 0.4%QDs (●) at 300 K obtained with a charging time of $t_C = 1$ s and a charging voltage of $\Delta V = +1$ V.

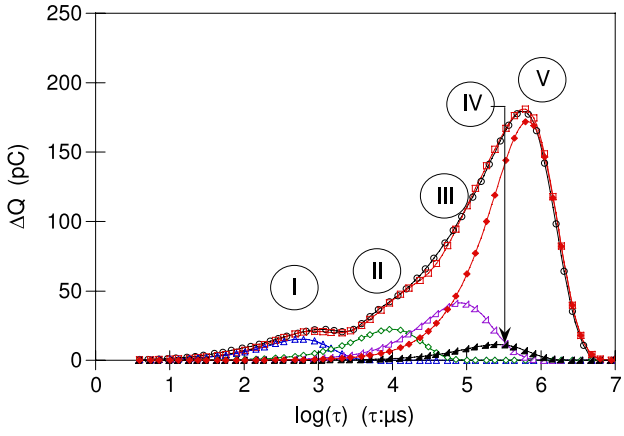

Figure 12. Resolved Q-DLTS spectrum recorded in an ITO/PEDOT/MEH-PPV + 0.4%QDs/Al diode using a charging voltage of $\Delta V = +1$ V and a charging time of $t_C = 1$ s, at 300 K.

additional trap level, created by the QDs. The trap parameters of the ITO/PEDOT:PSS/(MEH-PPV+QDs)/Al structures are displayed in table 1.

The most striking result obtained here is the decrease of density of the existing traps in MEH-PPV upon incorporation of QDs. In OLEDs, injected holes from the anode and electrons from the cathode recombine in the emitting layer and contribute to the luminescence of the devices. Generally, a low performance of OLEDs can be assigned to an imbalanced mobility of holes and electrons or to the presence of exciton quenching centers in the active layer. In the devices studied, we notice a decrease of current density and an increase of luminance when adding QDs to MEH-PPV. There are two possible causes for the observed modifications. First, a decrease in the current density may be assigned to an increase of trapping centers in the active layer, which is not observed in the Q-DLTS measurements. Indeed, QDs have introduced new traps in the polymer, but, as their concentration is low, their effects on the transport appear negligible. Previous results on CdSe QDs reported the existence of surface traps due to stoichiometric defects [36]. These traps include electron traps, which are shallow traps, and hole traps, which are deep traps. By comparing the activation energy values obtained in the composites and in CdSe QDs, it can be inferred that the type V traps of activation energy of ∼0.20 eV detected in composite films are due to surface traps of CdSe QDs. The second possible cause of the performance improvement is that aggregation of QDs can occur in the composites and this confines the injected holes and electrons between the polymer and QDs due to the lower LUMO and HOMO of QDs [37], favoring also their recombinations. Therefore, we tentatively propose the following scenario in the devices studied. Some of the QDs in the composite are dispersed within the volume of the film, and the remaining QDs aggregate to form small regions in the polymer films [38]. These QD islands are probably formed near the top of the spin-coated polymer layer during the drying process [39]. Such a formation is consistent with results obtained from electrical measurements on the one hand and with the light emission of the devices on the other hand. The dispersed nanoparticles in the MEH-PPV film would produce interactions with defects of the polymer chains, resulting in neutralization of these defects. Hence, fewer electrons or holes are trapped in the polymer matrix, and their recombination rate in the MEH-PPV/QDs composite increases, resulting in an improvement of the light emission from the polymer. On the other hand, aggregation of QDs in small islands in the polymer can confine the charge carriers in the vicinity of the QDs, resulting in a decrease of the current density. We interpret the modifications of the transport and of the EL in devices using composite materials by an increase of recombination rate of holes and electrons due to higher amounts of free charges present in the devices, which resulted from a reduction of the trapping centers by QDs.

4. Conclusion

In summary, we have fabricated and studied light-emitting diodes based on MEH-PPV blended with CdSe(ZnS) quantum dots. The luminance and efficiency of devices with QDs were found to be improved compared to those obtained in devices using the pristine polymer. The trap measurements revealed that, with QD incorporation, a new trap level is detected, which is attributed to defects of the nanoparticles. Furthermore, the density of the existing traps of the polymer decreased. We suggest that the dispersed QDs can inhibit the trapping centers, which are responsible for the quenching of luminescence. We also propose that aggregation of QDs could produce a blocking of carriers and increase the recombination of excitons. The results obtained in this work show the prime role of traps in charge carrier transport, which in turn impacts on the performance of devices. The role of the contact on the trap formation process is currently being investigated on devices with a Ca cathode, which provide higher performances than those obtained in devices with an Al cathode, and results will be published elsewhere.

Acknowledgment

The authors would like to thank Dr A M Marie (IMN) for performing the TEM analysis.

References

[1] Burroughes J H, Bradley D D C, Brown A R, Marks R N, MacKay K, Friend R H, Burn P L and Holmes A B 1990 *Nature* **347** 539
[2] Tang C W and VanSlyke S A 1987 *Appl. Phys. Lett.* **51** 913
[3] Friend R H *et al* 1999 *Nature* **397** 121
[4] Cao Y, Parker I D, Yu G, Zhang C and Heeger A J 1999 *Nature* **397** 414
[5] Peng X, Schlamp M C, Kadavanich A V and Alivisatos A P 1997 *J. Am. Chem. Soc.* **119** 7019
[6] Anikeeva P O, Halpert J E, Bawendi M G and Bulovic V 2007 *Nano Lett.* **7** 2196
[7] Murphy J E, Beard M C, Norman A G, Ahrenkiel S P, Johnson J C, Yu P, Micic O I, Ellingson R J and Nozik A J 2006 *J. Am. Chem. Soc.* **128** 3241
[8] Schaller R D, Petruska M A and Klimova V I 2005 *Appl. Phys. Lett.* **87** 253102
[9] Chaudhary S, Ozkana M and Chan W C W 2004 *Appl. Phys. Lett.* **84** 2925
[10] Yang H and Holloway P H 2003 *J. Phys. Chem.* B **107** 9705
[11] Dabbousi B O, Bawendi M G, Onitsukaa O and Rubner M F 1995 *Appl. Phys. Lett.* **66** 1316
[12] Zhao J, Bardecker J A, Munro A M, Liu M S, Niu Y, Ding I K, Luo J, Chen B, Jen A K Y and Ginger D S 2006 *Nano Lett.* **6** 463
[13] Park J H, Lim Y T, Park O O, Kim J K, Yu J W and Kim Y C 2004 *Chem. Mater.* **16** 688
[14] Choi S H, Song H, Park K, Yumb J H, Kimb S S, Lee S and Sung Y E 2006 *J. Photochem. Photobiol.* A **179** 135
[15] Wang P, Abrusci A, Wong H M P, Svensson M, Andersson M R and Greenham N C 2006 *Nano Lett.* **6** 1789
[16] Sun B, Marx E and Greenham N C 2003 *Nano Lett.* **3** 961
[17] Wang L, Liu Y, Jiang X, Qin D and Cao Y 2007 *J. Phys. Chem.* C **111** 9538
[18] Coe S, Woo W K, Steckel J S, Bawendi M and Bulovic V 2003 *Org. Electron.* **4** 123
[19] Tang A W, Teng F, Gao Y H, Li D, Zhao S L, Liang C J and Wang Y S 2007 *J. Lumin.* **122/123** 649
[20] Zhao J, Zhang J, Jiang C, Bohnenberger J, Basché T and Mews A 2004 *J. Appl. Phys.* **96** 3206
[21] Carter S A, Scott J C and Brock P J 1997 *Appl. Phys. Lett.* **71** 1145
[22] Zhang F, Xu Z, Zhao S, Liu L, Sun B and Pei J 2006 *Physica* B **381** 256
[23] Kim Y K, Lee K Y, Kwon O K, Shin D M, Sohn B C and Choi J H 2000 *Synth. Met.* **111/112** 207
[24] Chou C H, Wang H S, Wei K H and Huang J Y 2006 *Adv. Funct. Mater.* **16** 909
[25] Liu H W, Laskar I R, Huang C P, Cheng J A, Cheng S S, Luo L Y, Wang H R and Chen T M 2005 *Thin Solid Films* **489** 296
[26] Park J H, Park S I, Kim T H and Park O O 2007 *Thin Solid Films* **515** 3085
[27] Chen K B, Chen M H, Yang S H, Hsieh C H, Hsu C S, Chen C C and Chien H J 2006 *J. Polym. Sci.* A **44** 5378
[28] Pientka M, Dyakonov V, Meissner D, Rogach A, Talapin D, Weller H, Lutsen L and Vanderzande D 2004 *Nanotechnology* **15** 163
[29] Greenham N C, Peng X and Alivisatos A P 1996 *Phys. Rev.* B **54** 17628
[30] Polyakov V I, Rossukanyi N M, Rukovishnikov A I, Pimenov S M, Karabutov A V and Konov V I 1998 *J. Appl. Phys.* **84** 2882
[31] Farmer J W, Lamp C D and Meese J M 1982 *Appl. Phys. Lett.* **41** 1063
[32] Gaudin O, Jackman R B, Nguyen T P and Le Rendu P 2001 *J. Appl. Phys.* **90** 4196
[33] Nguyen T P, Le Rendu P, Gaudin O, Lee A J T, Jackman R B and Huang C H 2006 *Thin Solid Films* **511/512** 338
[34] Kažukauskas V 2004 *Semicond. Sci. Technol.* **19** 1373
[35] Stallinga P, Gomes H L, Rost H, Holmes A B, Harrison M G and Friend R H 2000 *Synth. Met.* **111/112** 535
[36] Lifshitz E, Dag I, Litvitn I D and Hodes G 1998 *J. Phys. Chem.* B **102** 9245
[37] Lee C W, Chou C H, Huang J H, Hsu C S and Nguyen T P 2008 *Mater. Sci. Eng.* B **147** 307
[38] Colvin V L, Schlamp M C and Alivisatos A P 1994 *Nature* **370** 354
[39] Coe S, Woo W K, Bawendi M and Bulovic V 2002 *Nature* **420** 800